

# Planar shock compression of single crystal tantalum from 6 – 23 GPa

**G Whiteman, S Case and J C F Millett**

AWE, Aldermaston, Reading, Berkshire, RG7 4PR, United Kingdom

E-mail: [glenn.whiteman@awe.co.uk](mailto:glenn.whiteman@awe.co.uk)

**Abstract.** Planar impact experiments have been performed to produce simultaneous shock loading of the three principal orientations of single crystal tantalum ([100], [110] and [111]) to peak stresses of 6 and 23 GPa. Results reveal that the [100] orientation exhibits the largest elastic limit. Shock velocity measurements indicate that for all of the materials, and most notably in the [100] orientation, there is a low stress excursion from a linear  $U_s$ - $u_p$  plot similar to that previously seen in polycrystalline tantalum. This suggests sensitivities at low stress which require further investigation. The experiments have been simulated using a single crystal plasticity finite element model that accounts for thermally-activated and drag-resisted dislocation motion, and for evolution of the dislocation density. The model is seen to qualitatively describe some of the features described above.

## 1. Introduction

The response of metals to shock loading is of significant interest to many research communities such as those of aerospace, automotive and defence. Accurate physics based material models are required in order to perform hydrocode calculations of complex dynamic loading scenarios which occur in those industries. To improve, develop and validate these models requires high fidelity data over a wide range of loading conditions and strain-rates. One particular avenue of our research is in the development and refinement of a Crystal Plasticity Finite Element Model (CPFEM). The metal tantalum (Ta) has been chosen for this model development as it has a body centred cubic (bcc) structure and there exists a significant amount of polycrystalline data already published in the literature. Dynamic loading data on single crystal Ta materials is however very limited, particularly within the longitudinal stress range discussed here ( $\leq 23$  GPa), where the data is required to present a stringent test of the CPFEM model.

## 2. Materials

The single crystal materials used in this research were in the form of three individual bars of pure Ta ( $> 99.99\%$ ), grown as  $\sim 14$  mm diameter bars with the axes parallel to the [100], [110] and [111] directions. Manufacture quoted mis-orientation was less than  $0.5^\circ$ . Ambient measured density ( $\rho_0$ ) for all samples was  $16.59 \pm 0.02$  g/cm<sup>3</sup>. Longitudinal and shear sound speeds ( $c_L$  and  $c_S$ ) were measured using pulse echo techniques for [100], [110] and [111] orientations respectively as;  $c_L$  - 4.018, 4.235, 4.300 mm/ $\mu$ s and  $c_S$  - 2.232, 2.237 (1.783) and 1.938 mm/ $\mu$ s. The two measurements shown for the shear velocity for the [110] orientation crystals are its maxima and minima which were measured as the transducer was rotated due to the 2-fold rotational symmetry of that orientation. These measured sound speeds are in agreement with those expected when using tabulated values for single crystal



elastic constants. Dislocation densities of the initial materials have been measured via transmission electron microscopy (TEM) techniques to be  $\sim 6 \times 10^8 \text{ cm}^{-2}$  for all three orientations.

### 3. Experiments

A series of four experiments have been fielded on the AWE 70 mm bore gas-gun. Each target contained four  $\sim 4 \text{ mm}$  thick targets; one sample of each single crystal orientation and one polycrystalline target (the polycrystalline data is not discussed within this paper). An approximately 3 mm thick polycrystalline Ta impact plate was used in each case. A diagram of the targets and experiment set up is given in figure 1. The impact velocities for experiments 1 to 4 were 212.2, 197.6, 726.2 and 730.8 m/s respectively. A frequency shifted Heterodyne Velocimetry (HetV) [1] system was used to measure the rear surface particle velocity on each of the four samples as well as the impactor velocity. A set of six ionization pins were mounted around the target on a 60 mm pitch centred diameter, flush with the impact surface in order to measure the impact time and tilt.

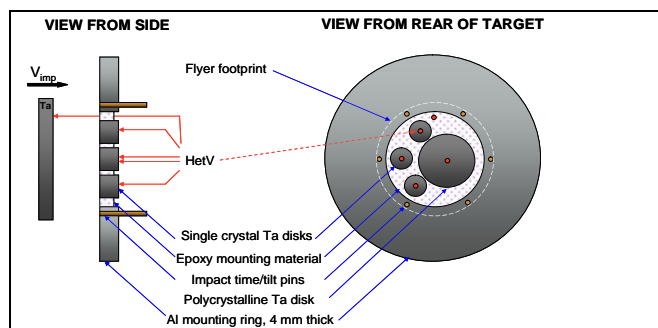


**Figure 1.** Schematic of the experimental set-up, target design and diagnostics for the single crystal Ta shock experiments.

## 4. Results

### 4.1. Velocimetry Data

The full set of rear surface velocity profiles were captured from the experiments, example data sets from experiments 1 and 3 are shown in figures 2 and 3 respectively. The traces are aligned such that impact time is set to the origin. Due to the small diameter of the single crystal targets the maximum achievable one-dimensional shock loading time (*i.e.* the time from initial motion until edge releases reach the recording position) is  $\sim 475$  and  $325 \text{ ns}$  for the 6 and 23 GPa experiments respectively.

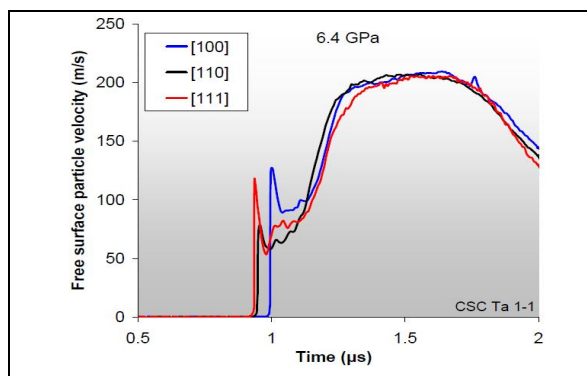


**Figure 2.** Rear free surface velocimetry for 6.4 GPa impact stress experiment.

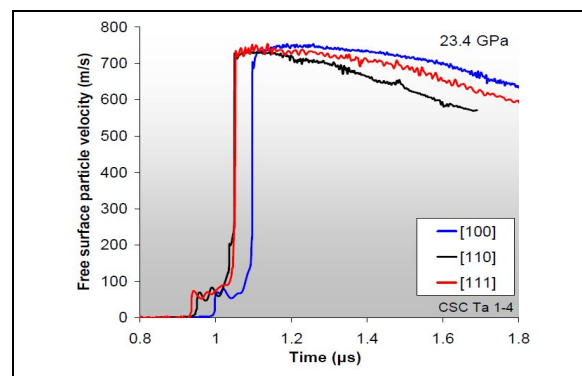


**Figure 3.** Rear free surface velocimetry for 23.4 GPa impact stress experiment.

All of the materials show a characteristic Hugoniot Elastic Limit (HEL) with a spike and relaxation to an approximate equilibrium level before the plastic shock arrival. This behaviour is thought to be due to initially low numbers of mobile dislocations making plastic flow difficult which gives an elastic overshoot. As plastic slip begins there is a growth of mobile dislocation density allowing the

dislocations to move at a lower average speed resulting in a reduction in the slip resistance and hence the relaxation as observed. The slow kinetics in some bcc materials (due to high Peierls stress [2]) means that this form is more evident in Ta than, for example, in face centered cubic materials.

The levels and qualities of the HEL and the wave speeds observed within all of the result show significant differences among the three materials. The nominally repeat experiments were consistent for the [110] and [111] oriented materials (accepting the slight differences in impact stress) although the [100] material showed a significant drop in the plastic wave arrival time for the small drop in the impact stress from 6.4 to 6.0 GPa. The maximum HEL peaks were measured to be 4.74, 2.89 and 4.19 GPa for [100], [110] and [111] orientations respectively, although for the high stress experiments the value of the absolute peak was lost due to low return signal strength levels in the HetV diagnostic (an experimental issue which will be eradicated on further experiments planned for the near future). The relaxed HEL values, taken as the extrapolation of the approximately level portion of the profile to the front of the elastic wave, were more consistent. The mean values for the three orientations were  $2.7 \pm 0.4$ ,  $1.9 \pm 0.1$  and  $2.2 \pm 0.2$  GPa for [100], [110] and [111] respectively.

There is a notable feature, shown in figure 3, where a kink appears on the shock rise portion of the [110] data. This feature, which was replicated on the repeat experiments, is unique to the [110] data and is not attributable to analytic errors or elastic reverberations and is discussed later.

#### 4.2. Modelling

These experiments are being used to validate a single crystal plasticity model. Plasticity in the model is assumed to be dominated by plastic slip that is mediated by the movement of crystal defects (dislocations). In this slip kinetics model, a scaling of the slip resistance that depends on pressure is included. The thermal activation model that describes resistance to dislocation motion at low and intermediate strain-rates is augmented by a dislocation drag model that accounts for mechanisms resistive to dislocation motion at the very high strain-rates encountered in shock deformation. So total dislocation velocity is given by,

$$v_{total}^{\alpha} = \left( v_{ta}^{\alpha-1} + v_{dd}^{\alpha-1} \right)^{-1} \quad (1)$$

where  $\alpha$  denotes slip system. The dislocation velocities in the thermal activation ('ta') and dislocation drag ('dd') regimes, which have been fitted to molecular dynamics (MD) data [3], are given (for bcc materials) by,

$$v_{ta}^{\alpha} = v_0 \left\{ \exp \left[ \frac{F_0}{kT} \left\langle 1 - \left\langle \frac{\tau_{eff}^{\alpha}}{\tau_0 (C_{44} / C_{44_0})} \right\rangle^p \right\rangle^q \right] - 1 \right\}^{-1} \quad (2)$$

$$v_{dd}^{\alpha} = \frac{b \tau_{eff}^{\alpha}}{D(C_{44} / C_{44_0})} \quad (3)$$

Here  $v_0$  is a parameterized reference velocity,  $F_0$  is the activation energy to overcome a Peierls barrier,  $T$  is temperature,  $k$  is Boltzmann's constant,  $p$  and  $q$  are temperature dependence fitting parameters,  $\tau_{eff}$  is the effective resolved shear stress on system  $\alpha$ ,  $\tau_0$  is the non-evolving Peierls resistance at 0 K (for bcc materials only),  $b$  is the Burgers vector,  $D$  is the drag coefficient and  $C_{ij}$  are the elastic moduli. The braces indicate that  $\langle x \rangle = x$  for  $x > 0$ , and  $\langle x \rangle = 0$  for  $x \leq 0$ . It is important for a physically predictive model that a physical description of the plastic strain-rate ( $\dot{\gamma}$ ) is used that depends on the average dislocation velocity ( $\bar{v}$ ) (and its dependence on stress-state, pressure and temperature) and dislocation density evolution ( $\dot{\rho}$ ) (and its dependence on strain-rate and plastic strain). *i.e.*

$$\dot{\gamma} = \rho_m b \bar{v} \quad (\text{the Orowan relation}) \quad (4)$$

where  $\rho_m$  is the mobile dislocation density. The model also describes both mobile and immobile dislocation density evolution on each slip system including terms of dislocation multiplication, annihilation and trapping although does not yet include nucleation or recovery terms. This density evolution description has currently been fitted to all of the shock data although direct linkage to molecular and dislocation dynamics will be undertaken in the future.

Figures 4 and 5 show examples of the model predictions of free surface velocity compared to data for a [100] crystal at 6.4 GPa and a [110] oriented crystal at 23.2 GPa. In general the model captures stress relaxation in the HEL and the elastic to plastic transition well indicating the mobile dislocation density evolution is being captured successfully. So far the model has not matched the relative HEL magnitudes between the three orientations although improvements are ongoing. Bringing in non-Schmidt stress effects [4] (*i.e.* slip rates not only dependant on resolved shear stress on each slip system which is likely in a bcc material) and introducing different dislocation properties on different slip systems such as the {110}<111>, {112}<111>, twin/anti-twin asymmetry could help in the future.

As previously noted there is an interesting feature on the shock rise portion of the [110] oriented crystal for the highest stress experiments, suggesting that an extra slip system may have been operated at this stress level. Evidence of this feature is also reproduced in the simulations as seen in figure 5. In the model this feature corresponds to activation of extra slip planes during shock rise due to the presence of a shear stress wave arising from the 2-fold rotational symmetry in [110] direction.

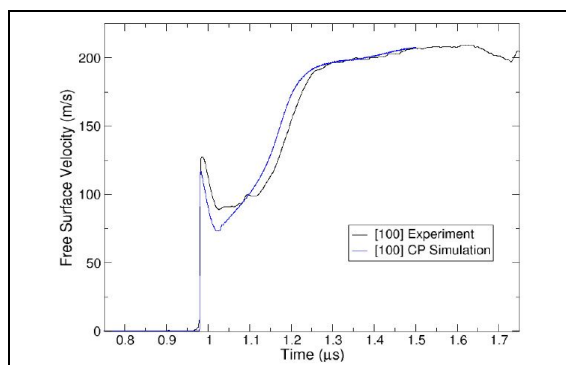


**Figure 4.** Comparison of CP simulation with experimental data for [100] crystal at 6.4 GPa.

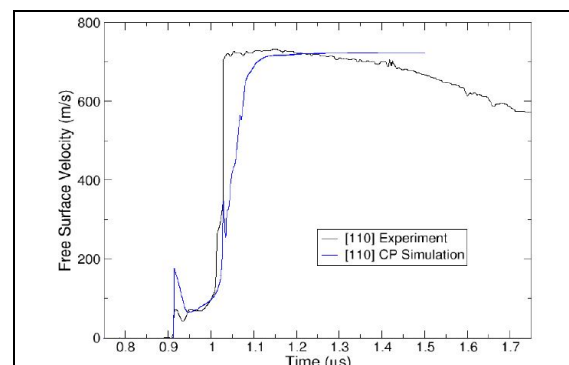


**Figure 5.** Comparison of CP simulation with experimental data for [110] crystal at 23.2 GPa.

## 5. Discussion and conclusions

As discussed previously there were significant variations in the observed peak elastic limits which is likely to be a response to minor impact tilt. Other more minor variations in the peak and lower limits could be an effect of variation of sub-grain misalignments as suggested in the ramp loaded experiments [5] although this has not yet been investigated for these materials. When the data is compared to the relevant ramp loading data in [100] and [110] oriented single crystal Ta the HEL values obtained are comparable. This suggests that the same deformation mechanisms are operating over a range of strain-rates (not a universal observation for all materials). The caveat to this observation is that the maximum peak elastic limit in the [100] orientation is higher than for the ramp loading experiments which suggests strain-rate effects which have yet to be explored. The ramp loading experiments are both at different strain-rate *and* pulse duration to these shock experiments, as such a more thorough comparison will require further shock research on ~ 1 mm thick samples. These experiments are planned for the near future and will also allow evidence of precursor decay and the degree of relaxation behind the elastic limit to be investigated. It is known that mobile dislocation density will effect precursor decay and also that interstitial content in Ta can significantly affect deformation behaviour above a few tens of parts per million [6]. TEM analysis has determined that the

dislocation density for this research increases from  $\sim 6 \times 10^8 \text{ cm}^{-2}$  (for all orientations initially) to  $\sim 2 \times 10^{10} \text{ cm}^{-2}$ ,  $4 \times 10^{10} \text{ cm}^{-2}$  and  $6 \times 10^{10} \text{ cm}^{-2}$  for the samples loaded along [100], [110] and [111], respectively. Analysis to determine interstitial content is ongoing at the time of writing.

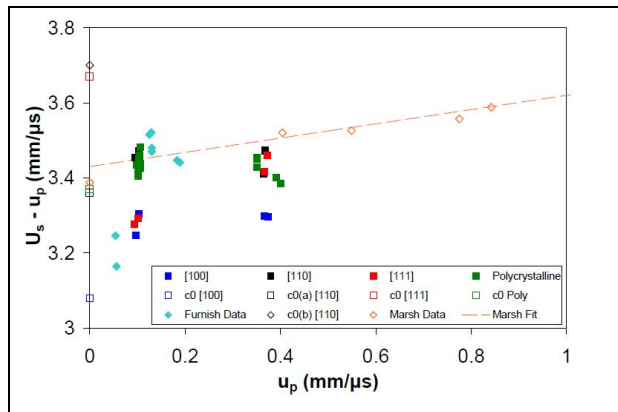


**Figure 6.** Plot of Hugoniot using measured shock and particle velocities from these experiments. Also shown is polycrystalline data from [7,8]

From the data obtained in these experiments Hugoniot points have been determined which are shown in figure 6 compared with polycrystalline data from Marsh [7], Furnish *et al.* [8] and also this current research. It is clear that the [100] orientation exhibits the lowest shock velocity with the [111] orientation only similar at low stresses. At high stress the [111] orientation is similar to the polycrystalline materials and [110] orientation. The polycrystalline material data from these experiments largely agrees with the  $\geq 8$  GPa stress data from [7-8]. It is noticeable however, that the lower stress,  $\sim 3.5$  GPa, data from [8] moves significantly off of the linear fit. Furnish *et al.* noted a similar discrepancy in another paper [9] suggesting crystallographic texture effects may be the cause. Fiske *et al.* [10] suggest that the discrepancy is more likely to arise from the assumption of a linear extrapolation of the shock velocity-particle velocity data gathered in the strong shock regime to the weak (two-wave) shock regime such that an unsteady plastic wave occurs. This appears to be corroborated by our results for the [111] orientation and also possibly the [100] orientation where the initially lower shock velocity (compared to the other materials) appears to rapidly decrease when our experiments moved from a shock stress of 6.4 to 6 GPa. It is reasonable to suggest that the variation of the non-linear/unsteady behaviour occurring in polycrystalline and single crystal Ta is related to crystallographic orientations and texture which might be expected to be more prevalent in a bcc material due to non-Schmidt behaviour. Further experiments at lower shock stresses are required to examine and characterise the non-linear shock velocity Hugoniot behaviour more fully.

The modelling work which has been undertaken so far has captured many of the key features of these experiments such as the peak and decay of the elastic limit, the elastic to plastic transition and the effects of the shear stress wave in the high stress [110] experiments. There are however still discrepancies, most notably in the relative magnitude of the peak elastic limits. This could be caused by a number of factors one of which is that the model currently assumes that slip rates depend only on the resolved shear stress on each slip system (the Schmid stress) whereas theoretical calculations in bcc materials have shown that the motion of dislocations is also dependent on additional stress components. The addition of dislocation nucleation mechanisms in the dislocation density evolution model may be required in order to better describe shock deformation at the upper end of the shock pressure range studied here. Their exclusion may explain the poorer prediction of the 23 GPa shock data in comparison to that at 6 GPa, as seen in figures 4 and 5.

The research presented in this paper represents a useful resource in the current and future development of CPFEM models. The observed responses to shock loading vary significantly among the three single crystals exhibiting resolvable distinctive features which provide advantageous evidence for comparison with the model. The model itself has so far proved to be of high quality indicating interesting successes such as the corroborative confirmation of the existence of the extra

shear wave seen in the [110] data. Further research is still required and is planned as discussed throughout this paper in order to allow us to further understand and predict the mechanisms at play in the dynamic deformation of the single crystal Ta materials.

## 6. Acknowledgements

This research was carried out with the assistance of several colleagues at AWE; V Durrant, P Keightley, M Lowe, G Owen, N Park and M Philpott. B Pang and I Jones of the School of Metallurgy and Materials, the University of Birmingham undertook the TEM of the samples and our thanks also go to D Eakins and D Chapman of the Institute of Shock Physics at Imperial College for useful discussions. © British Crown Owned Copyright 2013/AWE

## References

- [1] Strand O T, Goosman D R, Martinez C, Whitworth T L and Kuhlow W W 2006 Compact system for high-speed velocimetry using heterodyne techniques *Rev. Sci. Instrum.* **77** 083018
- [2] Millett J C F, Bourne N K, Park N T, Whiteman G and Gray III G T 2011 On the behaviour of body-centred cubic metals to one-dimensional shock loading *J. Mater. Sci.* **46** 3899-906
- [3] Barton N R, Bernier J V, Becker R, Arsenlis A, Cavallo R, Marian J, Rhee M, Park H-S, Remington B A and Olson R T 2011 A multiscale strength model for extreme loading conditions *J. Appl. Phys.* **109** 073501
- [4] Schmid E 1924 Yield point of crystals - critical shear stress law *Proc. of the 1<sup>st</sup> Int. Congress on Applied Mechanics* p342
- [5] Asay J R, Vogler T J, Ao T and Ding J L 2011. Dynamic yielding of single crystal Ta at strain rates of  $\sim 5 \times 10^5$  /s *J. Appl. Phys.* **109** 073507
- [6] Schwartz A J, Stölken J S, King W E, Campbell G H, Lassila D H, Shu J Y, Sun S and Adams B L 1998 Analysis of compression behavior of a [011] Ta single crystals with orientation imaging microscopy and crystal plasticity *MRS Proc.* **539** 221
- [7] Marsh S P 1980 *LASL Shock Hugoniot Data* (Los Angeles, University of California Press)
- [8] Furnish M D, Chhabildas L C and Steinberg D J 1994 Dynamical behaviour of tantalum *AIP Conf. Proc.* **309** 1099-1102
- [9] Furnish M D, Lassila D H, Chhabildas L C and Steinberg D J 1995. Dynamic material properties of refractory materials: tantalum and tantalum/tungsten alloys *AIP Conf. Proc.* **370** 527-530
- [10] Fiske P S, Holmes N and Lassila D 1999. Shock Loading of Ta: Yield and Hardening Behavior of Polycrystalline and Oriented Single Crystals *Proc. Plasticity* **7** 639-42